

LATERALLY BRACED COLD-FORMED STEEL FLEXURAL MEMBERS WITH EDGE STIFFENED FLANGES

By B. W. Schafer¹ and T. Peköz,² Members, ASCE

ABSTRACT: The moment capacity of a laterally braced cold-formed steel flexural member with edge stiffened flanges (e.g., a channel or zee section) may be affected adversely by local or distortional buckling. New procedures for hand prediction of the buckling stress in the local and distortional mode are presented and verified. Numerical investigations are employed to highlight postbuckling behavior unique to the distortional mode. Compared with the local mode, the distortional mode is shown to have (1) heightened imperfection sensitivity, (2) lower postbuckling capacity, and (3) the ability to control the failure mechanism even in cases when the elastic buckling stress in the local mode is lower than in the distortional mode. Traditional design methods do not explicitly recognize distortional buckling, nor do they account for the observed phenomena in this mode. A new design method that integrates distortional buckling into the unified effective width approach, currently used in most cold-formed steel design specifications, is presented. For each element a local buckling stress and a reduced distortional buckling stress are compared to determine the effective width. Comparison with experimental tests shows that the new approach is more consistent and reliable than existing design methods.

INTRODUCTION

Finite strip analysis of a flexural member with an edge stiffened flange (Fig. 1) reveals three fundamental buckling modes: local, distortional, and lateral-torsional. For a laterally braced flexural member the lateral-torsional buckling mode is restricted. Therefore, the two primary modes of concern are local and distortional buckling.

The American Iron and Steel Institute (AISI) Specification for the design of cold-formed steel structural members (AISI 1996), hereon referred to as the AISI specification, attempts to account for distortional buckling through an empirical reduction of the local plate buckling coefficient k . The empirical k values do not agree with the actual distortional buckling stress. The experimental work (Desmond et al. 1981) that was conducted to determine the empirical k expressions actually concentrated efforts on local buckling of the flange. This was accomplished by testing back-to-back sections. This experimental setup strongly restricts buckling in the web and hence distortional buckling as well. More recent experiments on laterally braced flexural members with edge stiffened flanges by Willis and Wallace (1990), Schuster (1992), Morayra (1993), and Ellifritt et al. (1997) demonstrate unconservative strength predictions using the AISI specification.

A hand method for the prediction of the distortional buckling stress in compression members was derived by Lau and Hancock (1987). Hancock extended this approach to flexural members in Hancock (1995, 1997). In Hancock et al. (1996) a method for evaluating the strength in distortional buckling is proposed. Hancock et al.'s method provides an independent strength calculation for distortional buckling. The suggested design strength is the minimum of the AISI specification method and a distortional buckling method. Comparison of this approach with test data is favorable, though the method proves overly conservative in many cases.

A unified treatment of local and distortional buckling in laterally braced flexural members with edge stiffened flanges is

the objective here. The procedure begins with closed-form prediction of the local and distortional buckling stresses. Interaction of the flange, web, and lip, in both local and distortional buckling, is considered. A need for the integration of the distortional mode into the design procedure is highlighted by two behavioral phenomena. First, the distortional mode has less postbuckling capacity than the local mode. Second, the distortional mode has the ability to control failure even when it occurs at a higher critical stress than the local mode. A design method incorporating these phenomena is needed to provide an integrated approach to strength prediction involving local and distortional buckling.

ELASTIC BUCKLING

Elastic buckling of cold-formed steel members can be predicted readily by numerical methods. However, for design purposes, closed-form solutions still are required. Therefore, new hand methods are developed for prediction of the buckling stress in the local and distortional modes.

LOCAL BUCKLING PREDICTION

An element model and a semiempirical interaction model are presented for closed-form approximation of the buckling stress in the local mode [see Fig. 1(a)]. The element model ignores interaction of the flange, web, and/or lip and treats the buckling of each element independently as is done in the current AISI specification. For instance, for a compression flange,

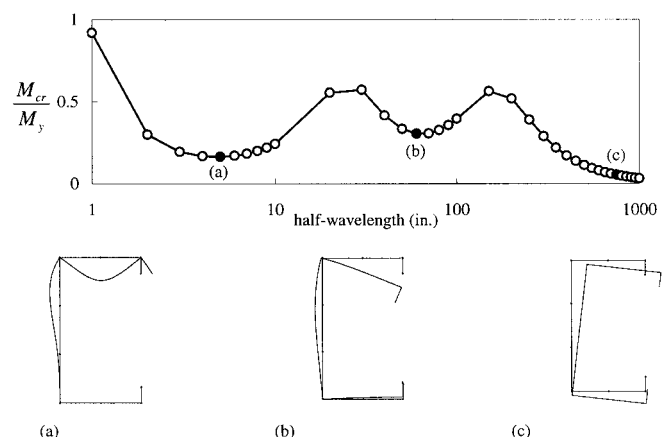


FIG. 1. Finite Strip Analysis of Flexural Member with Edge Stiffened Flange: (a) Local Buckling; (b) Distortional Buckling; (c) Lateral-Torsional Buckling

¹Sr. Engr., Simpson, Gumpertz & Heger, Inc., 297 Broadway Ave., Arlington, MA 02474; formerly, Instructor, Cornell Univ., Ithaca, NY 14853.

²Prof., Cornell Univ., 220 Hollister Hall, Ithaca, NY.

Note. Associate Editor: C. Dale Buckner. Discussion open until July 1, 1999. To extend the closing date one month, a written request must be filed with the ASCE Manager of Journals. The manuscript for this paper was submitted for review and possible publication on February 2, 1998. This paper is part of the *Journal of Structural Engineering*, Vol. 125, No. 2, February, 1999. ©ASCE, ISSN 0733-9445/99/0002-0118-0127/\$8.00 + \$.50 per page. Paper No. 17532.

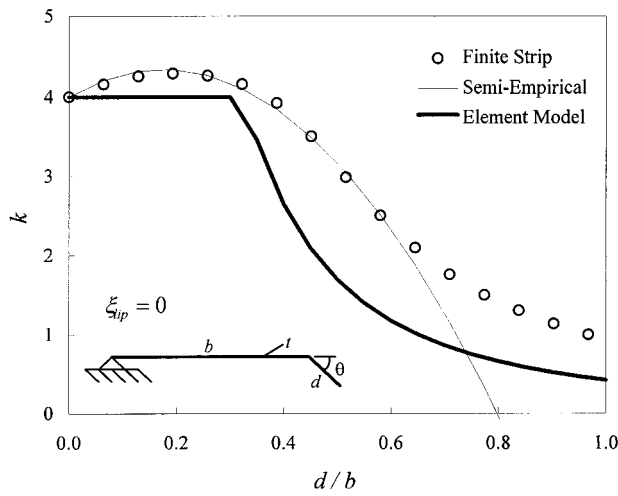


FIG. 2. Local Buckling of Isolated Flange and Lip

it is assumed that the element is simply supported on all four sides and thus a plate buckling coefficient of $k = 4$ is employed. For the semiempirical interaction model, local buckling of the flange is influenced by its attachment to a lip and a web.

Expressions for the plate buckling coefficients for the element model and the semiempirical interaction model follow. All of the k values are written in terms of the critical buckling stress of the flange, where

$$f_{cr} = k \frac{\pi^2 D}{b^2 t} \quad (1)$$

Several of the elements are subjected to a stress gradient, which is defined in terms of ξ

$$\xi = \frac{f_1 - f_2}{f_1} \quad (2)$$

where f_1 and f_2 = stresses at the opposite edges of the element. For the web, f_1 is at the web/compression flange juncture. For the lip, f_1 is at the lip/compression flange juncture. Compression stresses are positive (tension stresses negative).

Element model

$$\text{flange: } (f_{cr})_f \quad k = 4 \quad (3)$$

$$\text{web: } (f_{cr})_w \quad k = (0.5\xi_{web}^3 + 4\xi_{web}^2 + 4)(b/h)^2 \quad (4)$$

$$\text{lip: } (f_{cr})_l \quad k = k_{lip}(b/d)^2 \quad (5)$$

$$\text{for } 0 < \xi_{lip} \leq 1.1 \quad k_{lip} = 1.4\xi_{lip}^2 - 0.25\xi_{lip} + 0.425 \quad (6)$$

$$\text{for } 1.1 < \xi_{lip} \leq 2 \quad k_{lip} = 13\xi_{lip}^3 - 65.5\xi_{lip}^2 + 131\xi_{lip} - 80 \quad (7)$$

Semiempirical interaction model

$$\begin{aligned} \text{flange/lip: } (f_{cr})_{fl} \quad k &= (8.55\xi_{lip} - 11.07)(d/b)^2 \\ &+ (-1.59\xi_{lip} + 3.95)(d/b) + 4 \\ \text{for } \xi_{lip} \leq 1 \quad \text{and } d/b \leq 0.6 \end{aligned} \quad (8)$$

$$\text{flange/web: } (f_{cr})_{fw} \quad k = 1.125 \min\{4, (0.5\xi_{web}^3 + 4\xi_{web}^2 + 4)(b/h)^2\} \quad (9)$$

With the exception of the $k = 4$ solution, all of the foregoing expressions are new. The equations are determined by fitting expressions to finite strip analysis results. Fig. 2 shows the comparison for the local buckling expressions of an isolated flange and lip. The element model provides a lower bound, whereas the semiempirical interaction model closely approximates the finite strip analysis, within the prescribed parameters.

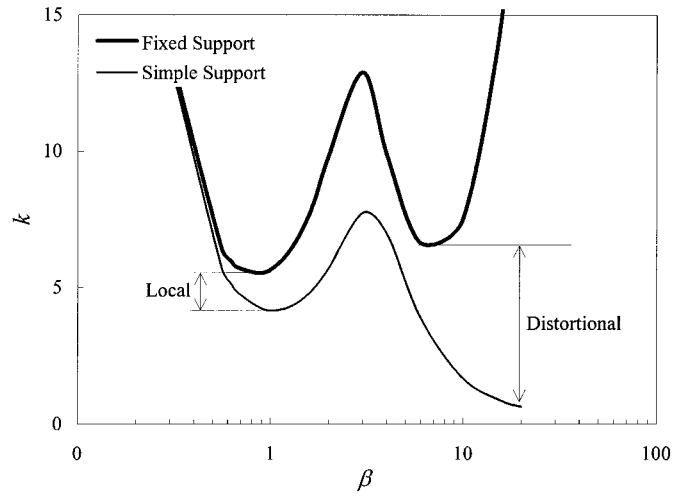


FIG. 3. Finite Strip Analysis of Isolated Flange and Lip

DISTORTIONAL BUCKLING PREDICTION

Prediction of distortional buckling, as shown in Fig. 1(b), is complicated because of the sensitivity to the solution to the rotational restraint at the web/compression flange juncture. Consider an isolated flange and lip (similar to the inset of Fig. 2) in which the web/flange juncture is idealized as either a simple support or a fixed support. Finite strip analysis (Fig. 3) shows that for local buckling the change in the plate buckling coefficient is small regardless of the boundary condition. However, for distortional buckling the potential differences are significant.

Closed-form prediction of the distortional buckling stress is based on an examination of the rotational restraint at the web/flange juncture. The rotational stiffness may be expressed as the summation of the elastic and stress-dependent geometric stiffness terms with contributions from both the flange and the web

$$k_{\phi} = (k_{\phi f} + k_{\phi w})_e - (k_{\phi f} + k_{\phi w})_g \quad (10)$$

Buckling ensues when the elastic stiffness at the web/flange juncture is eroded by the geometric stiffness, i.e.

$$k_{\phi} = 0 \quad (11)$$

Using (11) and writing the stress-dependent portion of the geometric stiffness explicitly

$$k_{\phi} = k_{\phi fe} + k_{\phi we} - f(\tilde{k}_{\phi fg} + \tilde{k}_{\phi wg}) = 0 \quad (12)$$

Therefore, the critical buckling stress (f) is

$$f = \frac{k_{\phi fe} + k_{\phi we}}{\tilde{k}_{\phi fg} + \tilde{k}_{\phi wg}} \quad (13)$$

Analytical models are needed for determining the rotational stiffness contributions from the flange and the web. For the flange, cross-sectional distortion is not important [Fig. 1(b)]; hence the flange is modeled as a column undergoing torsional-flexural buckling. This is similar to the approach of Sharp (1966), Lau (1988), Seah and Rhodes (1993), Davies and Jiang (1996), and Hancock (1997). For the web, cross-sectional distortion must be considered, so the web is modeled as a single finite strip. Therefore, the transverse shape function is a cubic polynomial. The longitudinal shape functions of the flange and web are matched by using a single half-sine wave for each.

Distortional Buckling—Model for the Flange

Consider the torsional-flexural buckling of a column with springs along one edge as shown in Fig. 4. The governing differential equations are

$$EI_{yf} \frac{d^4 u}{dz^4} + EI_{xyf} \frac{d^4 v}{dz^4} + P \left(\frac{d^2 u}{dz^2} + y_0 \frac{d^2 \phi}{dz^2} \right) + k_{xf}(u + (y_0 - h_y)\phi) = 0 \quad (14)$$

$$EI_{xf} \frac{d^4 v}{dz^4} + EI_{xyf} \frac{d^4 u}{dz^4} + P \left(\frac{d^2 v}{dz^2} - x_0 \frac{d^2 \phi}{dz^2} \right) + k_{yf}(v - (x_0 - h_x)\phi) = 0 \quad (15)$$

$$EC_{wf} \frac{d^4 \phi}{dz^4} - \left(GJ_f - \frac{I_{of}}{A_f} P \right) \frac{d^2 \phi}{dz^2} - P \left(x_0 \frac{d^2 v}{dz^2} - y_0 \frac{d^2 u}{dz^2} \right) + k_{xf}(u + (y_0 - h_y)\phi)(y_0 - h_y) - k_{yf}(v - (x_0 - h_x)\phi)(x_0 - h_x) + k_{\phi f} \phi = 0 \quad (16)$$

where I_{xf} , I_{yf} , I_{xyf} , I_{of} , C_{wf} , J_f , and A_f = section properties of the flange; k_{xf} , k_{yf} , and $k_{\phi f}$ = springs; x_0 and y_0 = distances from the centroid to the shear center; and h_x and h_y = distances from the centroid to the springs. The following shape functions, consistent with a simply supported column, are used:

$$\phi = A_1 \sin \left(\frac{\pi z}{L} \right), \quad u = A_2 \sin \left(\frac{\pi z}{L} \right) \quad (17a,b)$$

$$v = (x_0 - h_x) A_1 \sin \left(\frac{\pi z}{L} \right) \quad (17c)$$

For this application the k_{xf} spring stiffness is assumed zero and the k_{yf} spring stiffness is assumed infinite. The typical approach is to find the buckling load P_{cr} . However, the goal here is to write the solution in terms of the rotational restraint the flange provides at the web/flange juncture. The shape functions in (17) are substituted into (14)–(16) and the load P is written in terms of the uniform stress f_1 . If terms of order f^2 are neglected then the flange rotational restraint may be written in the linear form given in (12). The resulting rotational stiffness terms are

$$k_{\phi fe} = \left(\frac{\pi}{L} \right)^4 \left(EI_{xf}(x_0 - h_x)^2 + EC_{wf} - E \frac{I_{xyf}^2}{I_{yf}} (x_0 - h_x)^2 \right) + \left(\frac{\pi}{L} \right)^2 GJ_f \quad (18)$$

$$\tilde{k}_{\phi fg} = \left(\frac{\pi}{L} \right)^2 \left[A_f \left((x_0 - h_x)^2 \left(\frac{I_{xyf}}{I_{yf}} \right)^2 - 2y_0(x_0 - h_x) \left(\frac{I_{xyf}}{I_{yf}} \right) + h_x^2 + y_0^2 \right) + I_{xf} + I_{yf} \right] \quad (19)$$

For a simple lip stiffened flange (Fig. 4) the section properties in (18) and (19) are only a function of b , d , θ , and t

$$A_f = (b + d)t \quad (20)$$

$$J_f = 1/3bt^3 + 1/3dt^3 \quad (21)$$

$$I_{xf} = \frac{t(t^2b^2 + 4bd^3 - 4bd^3 \cos^2(\theta) + t^2bd + d^4 - d^4 \cos^2(\theta))}{12(b + d)} \quad (22)$$

$$I_{yf} = \frac{t(b^4 + 4db^3 + 6d^2b^2 \cos(\theta) + 4d^3b \cos^2(\theta) + d^4 \cos^2(\theta))}{12(b + d)} \quad (23)$$

$$I_{xyf} = \frac{tbd^2 \sin(\theta)(b + d \cos(\theta))}{4(b + d)} \quad (24)$$

$$I_{of} = \frac{tb^3}{3} + \frac{bt^3}{12} + \frac{td^3}{3} \quad (25)$$

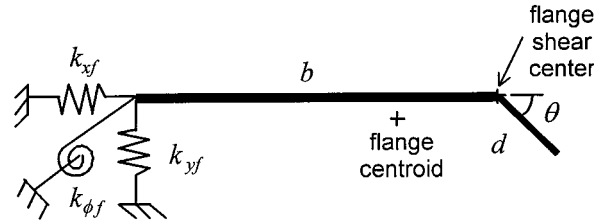


FIG. 4. Flange Model

$$x_0 = \frac{b^2 - d^2 \cos(\theta)}{2(b + d)} \quad (26)$$

$$h_y = y_0 = \frac{-d^2 \sin(\theta)}{2(b + d)} \quad (27)$$

$$h_x = \frac{-(b^2 + 2db + d^2 \cos(\theta))}{2(b + d)} \quad (28)$$

$$x_0 - h_x = b \quad (29)$$

$$C_{wf} = 0 \quad (30)$$

Distortional Buckling—Model for the Web

Derivation of the rotational restraint provided by the web to the web/flange juncture is based on using a single finite strip as shown in Fig. 5. The finite strip solution for the plate bending terms may be represented symbolically as

$$\begin{Bmatrix} \underline{F}_1 \\ \underline{M}_1 \\ \underline{F}_2 \\ \underline{M}_2 \end{Bmatrix} = \begin{bmatrix} k_{11} & k_{12} & k_{13} & k_{14} \\ k_{21} & k_{22} & k_{23} & k_{24} \\ k_{31} & k_{32} & k_{33} & k_{34} \\ k_{41} & k_{42} & k_{43} & k_{44} \end{bmatrix}_E \begin{Bmatrix} w_1 \\ \theta_1 \\ w_2 \\ \theta_2 \end{Bmatrix} - \begin{bmatrix} k_{11} & k_{12} & k_{13} & k_{14} \\ k_{21} & k_{22} & k_{23} & k_{24} \\ k_{31} & k_{32} & k_{33} & k_{34} \\ k_{41} & k_{42} & k_{43} & k_{44} \end{bmatrix}_G \begin{Bmatrix} w_1 \\ \theta_1 \\ w_2 \\ \theta_2 \end{Bmatrix} \quad (31)$$

where \underline{F} and \underline{M} = consistent nodal loads or moments; and k_{ij} = stiffness coefficients for the plate bending finite strip matrix [e.g., Cheung (1976)]. For simply supported edges, the terms of interest are

$$\begin{Bmatrix} \underline{M}_1 \\ \underline{M}_2 \end{Bmatrix} = \begin{bmatrix} k_{22} & k_{24} \\ k_{42} & k_{44} \end{bmatrix}_E - \begin{bmatrix} k_{22} & k_{24} \\ k_{42} & k_{44} \end{bmatrix}_G \begin{Bmatrix} \theta_1 \\ \theta_2 \end{Bmatrix} \quad (32)$$

To find $k_{\phi w}$, consider the strip to be unloaded along edge two and loaded along edge one (the web/compression flange juncture) with a sinusoidal edge moment of $M \sin(\pi y/L)$. The consistent nodal moments $\underline{M}_2 = 0$ and $\underline{M}_1 = 1/2ML$ are substituted. The solution then is written in terms of θ_1 . If $\theta_1 = 1$, then $M = k_{\phi w}$; therefore

$$k_{\phi w} = \frac{2}{L} \left((k_{22e} - k_{22g}) - \frac{(k_{24e} - k_{24g})(k_{42e} - k_{42g})}{(k_{44e} - k_{44g})} \right) \quad (33)$$

The web rotational stiffness $k_{\phi w}$ is decomposed into elastic and geometric parts

$$k_{\phi w} = k_{\phi we} - k_{\phi wg} \quad (34)$$

$$k_{\phi we} = \frac{2}{L} \left(k_{22e} - \frac{k_{24e}^2}{k_{44e}} \right) \quad (35)$$

$$-k_{\phi wg} = \frac{2}{L} \left(\left((k_{22e} - k_{22g}) - \frac{(k_{24e} - k_{24g})(k_{42e} - k_{42g})}{(k_{44e} - k_{44g})} \right) - \left(k_{22e} - \frac{k_{24e}^2}{k_{44e}} \right) \right) \quad (36)$$

The k_{ij} terms may be substituted directly to yield the com-

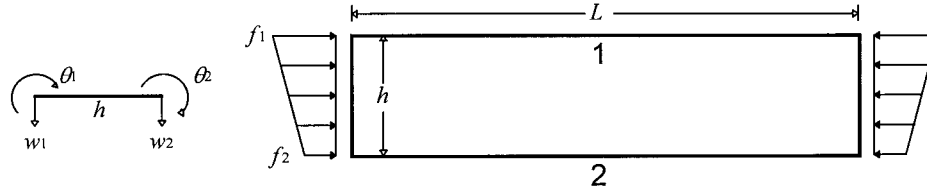


FIG. 5. Finite Strip Idealization of Web

plete analytical expressions for k_{ϕ} . Although exact, the expressions have an inordinate number of terms. Simplifications are made to provide a more compact solution. The elastic rotational stiffness in (35) is truncated by converting to partial fractions on the length L and keeping the constant term, the $1/L^2$ term, and the $1/L^4$ term. The resulting expression asymptotes to the full expression and provides a reasonable approximation of the elastic rotational stiffness

$$k_{\phi we} = D \left(\frac{3}{h} + \left(\frac{\pi}{L} \right)^2 \frac{19h}{60} + \left(\frac{\pi}{L} \right)^4 \frac{h^3}{240} \right) \quad (37)$$

For the geometric rotational stiffness in (36) the first approximation made is to linearize the stress f_1 . This is adequate for stress gradients near pure bending ($\xi_{web} \sim 2$), but breaks down as the stress approaches pure compression ($\xi_{web} = 0$). With this simplification, the geometric rotational stiffness takes the form

$$-k_{\phi wg} = \frac{2f_1}{L} \left(\frac{2k_{22e}k_{24e}k_{24g} - k_{22g}k_{24e}^2 - k_{22g}k_{22e}^2}{k_{22e}^2} \right) \quad (38)$$

Further simplification is provided after substituting in the k_{ij} terms by converting the solution to partial fractions on the length L . The general expression is then expressed in three terms, in which the dominators are

$$\frac{1}{L^2} + \frac{1}{(h^4 + L^2h^2 + L^4)} + \frac{1}{(h^4 + L^2h^2 + L^4)^2} \quad (39)$$

Parametric analysis shows the final term to be insignificant; thus it is neglected. The first two terms are combined to form the approximation of the rotational geometric stiffness, where

$$k_{\phi w} = k_{\phi we} - f_1 \tilde{k}_{\phi wg} \quad (40)$$

$$\tilde{k}_{\phi wg} = \frac{ht\pi^2}{13440} \{ [(45360(1 - \xi_{web}) + 62160)(L/h)^2 + 448\pi^2] \\ + (h/L)^2(53 + 3(1 - \xi_{web}))\pi^4 / [\pi^4 + 28\pi^2(L/h)^2] \\ + 420(L/h)^4 \} \quad (41)$$

Distortional Buckling—Critical Length

The buckling stress is a function of length L ; hence to approximate the L at which f is a minimum, the rotational stiffness terms are written explicitly in terms of L

$$k_{\phi fe} = (1/L)^4 C_1 + (1/L)^2 C_2 \quad (42)$$

$$\tilde{k}_{\phi fg} = (1/L)^2 C_3 \quad (43)$$

$$k_{\phi we} = K_1 + (1/L)^2 K_2 + (1/L)^4 K_3 \quad (44)$$

$$\tilde{k}_{\phi wg} = K_4(f(L)) \quad (45)$$

This gives the solution for the distortional buckling stress f as

$$f = \frac{(1/L)^4 C_1 + (1/L)^2 C_2 + K_1 + (1/L)^2 K_2 + (1/L)^4 K_3}{(1/L)^2 C_3 + K_4(f(L))} \quad (46)$$

The critical length is found by minimizing f with respect to

L . This minimization is complicated by the K_4 term—the web geometric stiffness. If the $f(L)$ in the K_4 term is approximated as $1/L^2$ then the C_3 and K_4 terms drop out. This assumption is made; therefore, the general solution for L_{cr} is

$$\frac{df}{dL} = 0 \rightarrow L_{cr} = \left(\frac{C_1 + K_3}{K_1} \right)^{1/4} \quad (47)$$

The appropriate terms for C_1 , K_3 , and K_1 are substituted, resulting in

$$L_{cr} = \left(\frac{4\pi^4 h(1 - \nu^2)}{t^3} \left(I_{xf}(x_0 - h_x)^2 + C_{wf} - \frac{I_{xyf}^2}{I_{yf}} (x_0 - h_x)^2 \right) \right. \\ \left. + \frac{\pi^4 h^4}{720} \right)^{1/4} \quad (48)$$

If the flange is assumed to be pinned [as is done in the critical length derivation of Lau (1988)] then the $(I_{xyf})^2/I_{yf}$ term is assumed negligible.

Elastic Distortional Buckling—Summarized

To find the critical buckling stress in the distortional mode (f_{cr})_{dist}, use (13). The rotational stiffness terms in (13) are found in (18), (19), (37), and (41). The rotational stiffness terms should be evaluated at L_{cr} via (48) unless $L_b < L_{cr}$.

COMPARISON OF ELASTIC BUCKLING METHODS

Thirty-two members are examined via finite strip analysis to compare with the proposed hand methods. The critical local buckling moment (M_{local}) and critical distortional buckling moment (M_{dist}) are recovered from the finite strip analysis. The geometry of the studied members is summarized in Table 1 and the comparison of the predictions is shown in Table 2.

TABLE 1. Geometry of Members

h (1)	b (2)	d (3)	θ (4)
50	25	6.25, 12.5	45, 90
100	25	6.25, 12.5	45, 90
	50	6.25, 12.5, 25	45, 90
150	25	6.25, 12.5	45, 90
	50	6.25, 12.5, 25	45, 90
	75	6.25, 12.5, 25, 37.5	45, 90
200	25	6.25, 12.5	45, 90
	50	6.25, 12.5, 25	45, 90
	75	6.25, 12.5, 25, 37.5	45, 90
	100	6.25, 12.5, 25, 37.5, 50	45, 90

TABLE 2. Performance of Elastic Buckling Methods

Statistics (1)	LOCAL BUCKLING		DISTORTIONAL BUCKLING
	Element Model	Interaction Model	Proposed method
	$M_{predicted}/M_{local}$ (2)	$M_{predicted}/M_{local}$ (3)	$M_{predicted}/M_{dist}$ (4)
Average	0.74	0.90	0.95
Standard deviation	0.12	0.05	0.08

TABLE 3. Geometry of Edge Stiffened Flanges

b/t (1)	d/t (2)	θ (3)	$\frac{P_{cr,local}}{P_{cr,dist}}$ (4)
25	4.00–19.0	90	1.82–0.25
	6.25–12.5	45	19.4–0.96
50	5.00–25.0	90	1.58–0.27
	6.25–25.0	45	1.76–0.51
75	6.25–37.5	90	1.34–0.18
	6.25–37.5	45	1.73–0.35
100	6.25–50.0	90	1.40–0.14
	6.25–50.0	45	1.75–0.23

The models proposed for the local buckling stress in (3)–(9) do not directly provide a direct prediction of the critical buckling moment. For the element model the governing local buckling stress is assumed to be the minimum of the flange, web, or lip. For the interaction model the governing local buckling stress is assumed to be the minimum of the flange/lip and flange/web calculation. The governing local buckling stress then is used to determine the local buckling moment.

For local buckling prediction the interaction model performs markedly better than the element model. The overly conservative nature of the element model is driven largely by poor predictions when the lip controls the local buckling stress. In cases when the lip controls, the average $M_{predicted}/M_{local}$ ratio is 0.6. The proposed distortional buckling method compares favorably with the finite strip analysis. Predictions for the $\theta = 45^\circ$ members are slightly less conservative than for the $\theta = 90^\circ$ members. Fortunately, the ratio for the $\theta = 45^\circ$ degree members is still 0.98 and the standard deviation is lower than for the $\theta = 90^\circ$ members.

POSTBUCKLING BEHAVIOR OF EDGE STIFFENED ELEMENTS

To investigate the postbuckling behavior in the local and distortional modes, nonlinear finite-element analysis of isolated flanges is completed using ABAQUS (Hibbitt, Karlsson & Sorensen, Inc. 1995). The flange is modeled as fixed at the web/flange juncture and nine node shell elements (S9R5) are employed. The material model is elastic-plastic with strain hardening. Initial imperfections in the local and distortional mode are superposed to form the initial imperfect geometry.

A longitudinal through thickness flexural residual stress of 30% f_y also is modeled.

The geometry of the members investigated is summarized in Table 3. The thickness is 1 mm and $f_y = 345$ MPa. Based on the displaced shape and location of plasticity two basic failure mechanisms from the finite element analysis are identified. It is observed that the final failure mechanism is consistent with the distortional mode even in cases when the distortional buckling stress is higher than the local buckling stress. Consider Fig. 6, which shows the final failure mechanism for all the members studied. Based solely on elastic buckling, one would expect the local buckling mode to control in all cases in which $(f_{cr})_{local}/(f_{cr})_{dist} < 1$; as the figure shows, this is not the case.

Finite element analysis also reveals that the postbuckling capacity in the distortional mode is less than that in the local mode. Consider Fig. 7, for the same slenderness values the distortional failures exhibit a lower ultimate strength. Similar loss in strength is observed experimentally and summarized in Hancock et al. (1994).

The geometric imperfections are modeled as a superposition of the local and distortional buckling modes. The magnitude of the imperfection is selected based on the statistical summary provided in Schafer and Peköz (1998). The error bars in Fig. 7 demonstrate the range of strengths predicted for imperfections varying over the central 50% portion of expected imperfection magnitudes. The greater the error bars, the greater the imperfection sensitivity.

The percent difference in the strength over the central 50% portion of expected imperfection magnitudes is used as a measure of imperfection sensitivity

$$\frac{(f_u)_{25\%imp} - (f_u)_{75\%imp}}{\frac{1}{2}((f_u)_{25\%imp} + (f_u)_{75\%imp})} \times 100\% \quad (49)$$

A contour plot of this imperfection sensitivity statistic (49) is shown in Fig. 8. Stocky members prone to failure in the distortional mode have the greatest sensitivity. In general, distortional failures are more sensitive to initial imperfections than local failures. Areas of imperfection sensitivity risk are assigned.

DESIGN OF FLEXURAL MEMBERS

The current AISI specification approach for the capacity of a laterally braced flexural member involves determining an

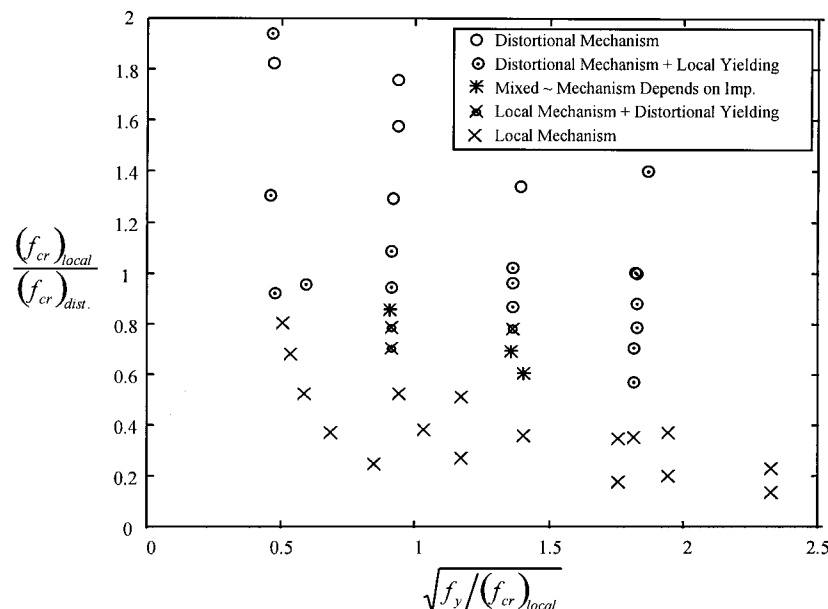


FIG. 6. Failure Mode of Edge Stiffened Flanges

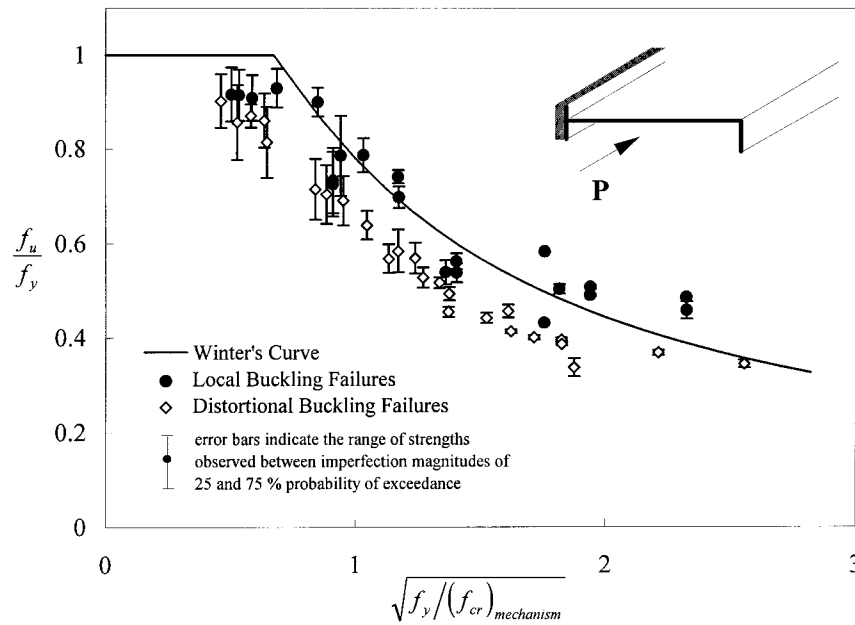


FIG. 7. Postbuckling Capacity of Edge Stiffened Flanges

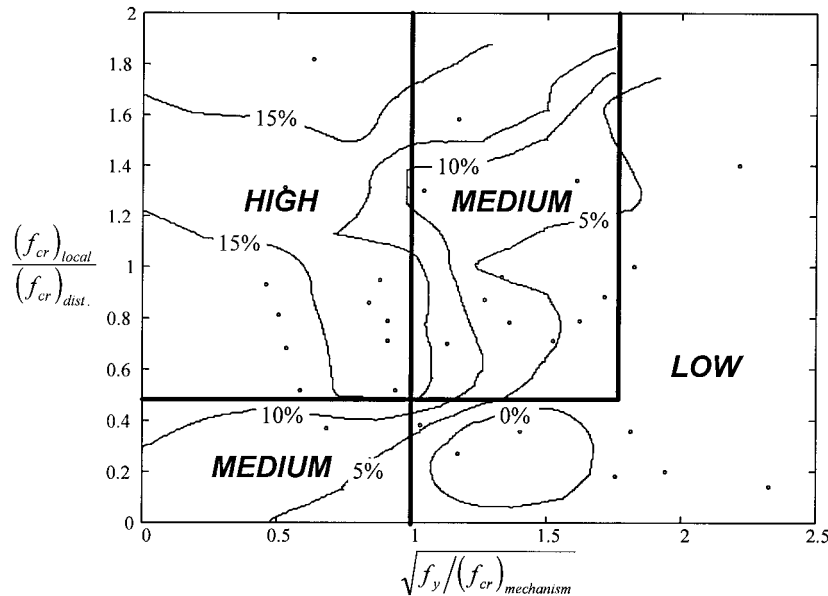


FIG. 8. Imperfection Sensitivity of Edge Stiffened Flanges

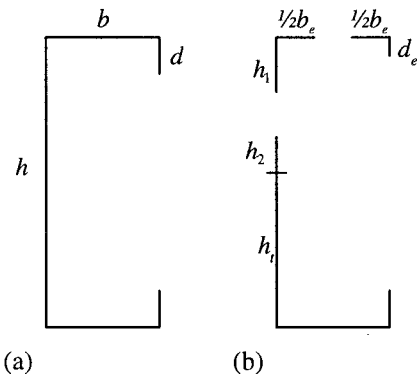


FIG. 9. Typical (a) Gross and (b) Effective Sections

effective section modulus to account for local buckling. As shown in Fig. 9, each element is reduced from its gross width (e.g., b) to an effective width (e.g., b_e). The reduction is based on an empirical correction to the work of von Kármán et al. (1932) completed by Winter (1947). The extension of this ap-

proach to all members of the cross section is based on the unified effective width approach of Peköz (1987). Once the effective width is calculated, determination of the flexural strength becomes a relatively straightforward manner, as shown in Table 4.

Design—Effective Width of Elements

The effective width of the flange (or lip, replace b with d) is

$$b_e = \rho b \quad (50)$$

where ρ is defined as

$$\rho = (1 - 0.22/\lambda)/\lambda \quad \text{for } \lambda > 0.673 \quad \text{otherwise } \rho = 1 \quad (51)$$

The slenderness parameter λ is

$$\lambda = \sqrt{f_y/(f_{cr})_{\text{flange}}} \quad (52)$$

Portioning of the effective width for the flange is simple (Fig. 9). However, in the case of a stiffened element under a

TABLE 4. Example for Effective Section Calculation

Element (1)	A (2)	y (3)	Ay (4)	Ay ² (5)	I _{own} (6)
Compression flange	b _t t	—	—	—	—
Web 1	h ₁ t	h ₁ /2	(h ₁) ² t/2	(h ₁) ³ t/4	t(h ₁) ³ /12
Web 2	h ₂ t	h - (h ₁ + h ₂)/2	—	—	—
Web 3	h ₃ t	h - (h ₁ /2)	—	—	—
Tensor flange	bt	h	—	—	—
Compression lip	d _t t	d _t /2	—	—	—
Tensor lip	dt	h - d/2	—	—	—
	Σ A		Σ Ay	Σ Ay ²	Σ I _{own}

$$M_n = S_{eff} f_1 S_{eff} = \frac{I_{eff}}{y_{eff}} y_{eff} = \frac{\sum Ay}{\sum A} I_{eff} = \sum Ay^2 + \sum I_{own} - \left(\sum A \right) y_{eff}^2$$

stress gradient (i.e., the web), the portioning of h to h_1 , h_2 , and h_3 is not straightforward. The expressions currently used in the AISI specification for a stiffened element under a stress gradient are discontinuous (Cohen 1987) and unconservative (Fig. 10). Other specifications, such as the Canadian standard for cold-formed steel structural members (Canadian Standards Association 1994), yield results more consistent with numerical analysis.

A new approach is proposed for the effective width of stiffened elements under a stress gradient (i.e., webs). Consider the effective width of an element in pure compression as shown in Fig. 11. Determination of the effective width is based on (1) an approximation of the nonlinear postbuckling stress via ρ and (2) a force balance between the approximated nonlinear stress and the effective section. For an element under a stress gradient (Fig. 11) the natural extension to this methodology is to determine the effective width by insuring that both a force and a moment balance are maintained between the approximated nonlinear stress and the effective section. The solution of this force and moment balance result in the following expressions:

$$h_1 = h\omega/\xi_{web} \quad \text{for } \xi_{web} > 0 \quad (53)$$

$$h_2 = (h/\xi_{web})\sqrt{\omega^2 - 2\omega + \rho} \quad \text{for } \xi_{web} > 0 \quad (54)$$

$$\lambda = \sqrt{f_y/(f_{cr})_{web}} \quad (55)$$

$$\rho = (1 - 0.22/\lambda)/\lambda, \quad \text{for } \lambda > 0.673, \quad \text{else } \rho = 1 \quad (56)$$

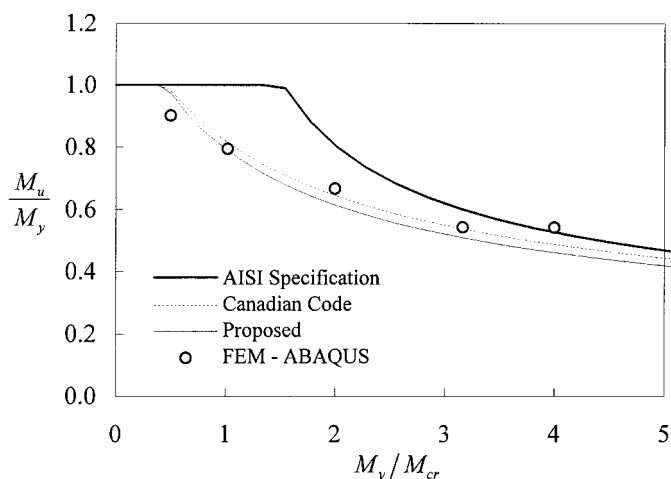


FIG. 10. Simply Supported Plate in Pure Bending

$$0 \leq \rho < 0.77 \quad \omega = 0.30\rho \quad (57a)$$

$$0.77 \leq \rho < 0.95 \quad \omega = 0.23 \quad (57b)$$

$$0.95 \leq \rho \leq 1.00 \quad \omega = -4.6\rho + 4.6 \quad (57c)$$

The resulting expressions agree with numerical analysis (Fig. 10). Further, the effective width of the web is a function of ρ . Thus, for the first time, the effective width of an element under a stress gradient is a function of the degree of nonlinearity in the postbuckling stress distribution, as reflected through ρ .

Design—Integrating Distortional Buckling into Procedure

If distortional buckling is considered then the critical buckling stress of an element (flange, web, or lip) is no longer solely dependent on local buckling. To properly integrate distortional buckling, reduce postbuckling capacity in the distortional mode and the ability of the distortional mode to control the failure mechanism even when at a higher buckling stress than the local mode must be incorporated. Consider defining the critical buckling stress of the element used in (52) or (55) as

$$(f_{cr}) = \min[(f_{cr})_{local}, R_d(f_{cr})_{dist}] \quad (58)$$

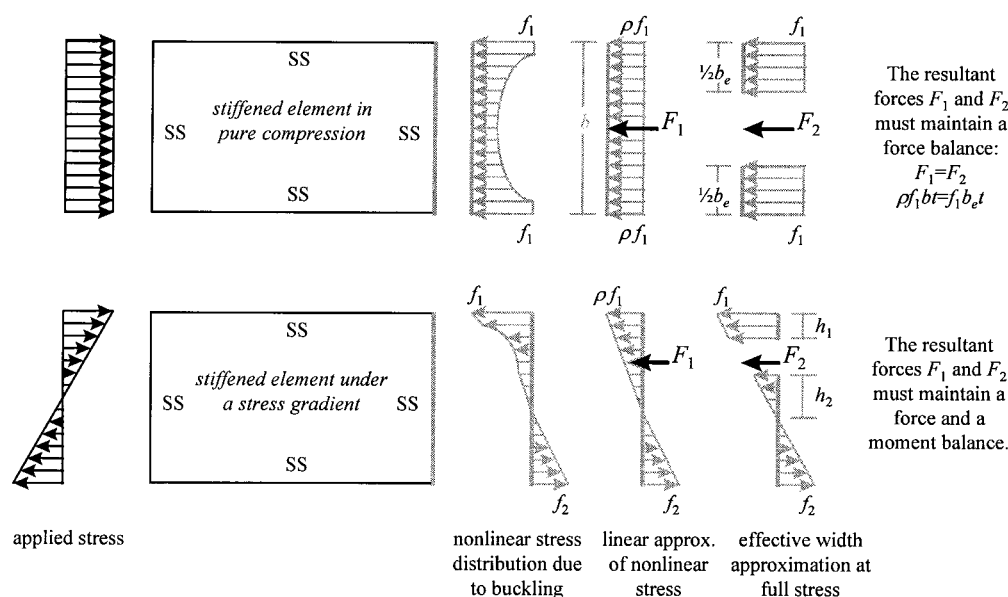


FIG. 11. Effective Width Determination

TABLE 5. Elastic Buckling Stress Determination

Model 1 $\sim M_1$ (no local buckling interaction)	Model 2 $\sim M_2$ (local interaction included)
$(f_{cr})_{web} = \min[(f_{cr})_w, R_d(f_{cr})_d]$	$(f_{cr})_{web} = \min[(f_{cr})_{fw}, R_d(f_{cr})_d]$
$(f_{cr})_{flange} = \min[(f_{cr})_f, R_d(f_{cr})_d]$	$(f_{cr})_{flange} = \min[(f_{cr})_{fw}, (f_{cr})_f, R_d(f_{cr})_d]$
$(f_{cr})_{lip} = \min[(f_{cr})_l, R_d(f_{cr})_d]$	$(f_{cr})_{lip} = \min[(f_{cr})_l, R_d(f_{cr})_d]$

For strength, if the reduced distortional mode governs, then (51) or (56) become

$$\rho = \sqrt{R_d}(1 - 0.22\sqrt{R_d}/\lambda)/\lambda \quad (59)$$

For $R_d < 1$, this method provides an additional reduction on the postbuckling capacity. Further, the method also allows the distortional mode to control in situations when the distortional buckling stress is greater than the local buckling stress. Thus, R_d provides a framework for solving the problem of predicting the failure mode and reducing the postbuckling capacity in the distortional mode. The selected form for R_d based on Figs. 6 and 7 and the experimental results of Hancock et al. (1994) is

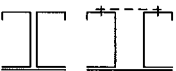

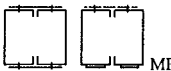
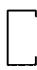
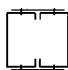
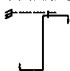
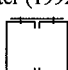
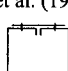
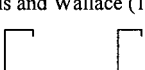
$$R_d = \min \left(1, \frac{1.17}{\lambda_d + 1} + 0.3 \right) \quad \text{where} \quad \lambda_d = \sqrt{f_y/(f_{cr})_{dist}} \quad (60)$$

Two models are advanced for predicting the critical buckling stress of the elements. The models are summarized in Table 5. With f_{cr} of the element known, the effective width of each element may be determined readily. The procedure outlined in Table 4 is completed to calculate the section capacity.

Comparison with Experimental Data

Experimental tests on laterally braced flexural members with edge stiffened flanges from Winter (1947), Desmond et al. (1981), LaBoube and Yu (1978), Schardt and Schrade (1982), Elhouar and Murray (1985), Cohen (1987), Willis and Wallace (1990), Ellifritt et al. (1992, 1997), Schuster (1992), Moreyra (1993), Shan et al. (1994), and Rogers and Schuster (1995) are gathered and examined. Based on the information available from the tests, the type of sections tested, and the loading arrangement, the applicability for use in this comparison is assessed. The experimental data of Winter (1947), Desmond (1978), Elhouar and Murray (1985), and Ellifritt et al.

TABLE 6. Summary of Test to Predicted Ratios

Researcher and the basic geometry/setup				$\frac{M_{test}}{M_{AISI}}$ $\frac{M_{test}}{M_1}$ $\frac{M_{test}}{M_2}$			
		max	min				
Cohen (1987) 	h/t	128	78	Avg.	1.08	1.02	1.02
	b/t	55	33	St. Dev.	0.05	0.11	0.11
	d/t	16	9	min	0.99	0.93	0.92
	$\sqrt{f_y/(f_{cr})_d}$	1.3	0.4	n<1 of 18	2	6	5
Ellifritt et al. (1997) 	h/t	139	113	Avg.	0.78	0.91	0.91
	b/t	48	31	St. Dev.	0.10	0.11	0.11
	d/t	16	11	min	0.61	0.75	0.75
	$\sqrt{f_y/(f_{cr})_d}$	1.5	1.2	n<1 of 10	10	8	8
Laboube and Yu (1978) 	h/t	269	77	Avg.	1.02	1.07	1.11
	b/t	75	28	St. Dev.	0.08	0.08	0.10
	d/t	15	11	min	0.87	0.88	0.92
	$\sqrt{f_y/(f_{cr})_d}$	1.2	0.7	n<1 of 32	11	7	6
Moreyra (1993) 	h/t	124	120	Avg.	0.86	0.96	0.99
	b/t	36	34	St. Dev.	0.08	0.11	0.09
	d/t	16	12	min	0.80	0.86	0.91
	$\sqrt{f_y/(f_{cr})_d}$	1.0	0.6	n<1 of 6	5	5	5
Rogers (1995) 	h/t	228	53	Avg.	1.02	1.09	1.11
	b/t	61	15	St. Dev.	0.11	0.07	0.07
	d/t	34	3	min	0.83	0.94	0.94
	$\sqrt{f_y/(f_{cr})_d}$	1.8	0.5	n<1 of 49	26	6	2
Schardt and Schrade (1982) 	h/t	183	178	Avg.	1.05	1.05	1.09
	b/t	71	45	St. Dev.	0.10	0.09	0.08
	d/t	16	10	min	0.89	0.92	0.96
	$\sqrt{f_y/(f_{cr})_d}$	1.4	0.6	n<1 of 37	14	13	7
Schuster (1992) 	h/t	168	166	Avg.	0.82	0.97	1.01
	b/t	34	33	St. Dev.	0.04	0.05	0.05
	d/t	11	10	min	0.78	0.93	0.97
	$\sqrt{f_y/(f_{cr})_d}$	1.0	1.0	n<1 of 5	5	3	3
Shan et al. (1994) 	h/t	256	43	Avg.	0.97	0.97	1.04
	b/t	58	19	St. Dev.	0.13	0.10	0.09
	d/t	20	6	min	0.75	0.79	0.85
	$\sqrt{f_y/(f_{cr})_d}$	1.0	0.4	n<1 of 29	18	22	10
Willis and Wallace (1990) 	h/t	131	126	Avg.	1.02	1.02	1.08
	b/t	40	38	St. Dev.	0.08	0.07	0.08
	d/t	17	14	min	0.92	0.93	0.98
	$\sqrt{f_y/(f_{cr})_d}$	0.7	0.6	n<1 of 4	2	1	1
All Experimental Data	h/t	269	43	Avg.	1.00	1.04	1.07
	b/t	75	15	St. Dev.	0.10	0.08	0.08
	d/t	34	3	min	0.61	0.75	0.75
	$\sqrt{f_y/(f_{cr})_d}$	1.8	0.4	n<1 of 190	93	71	47

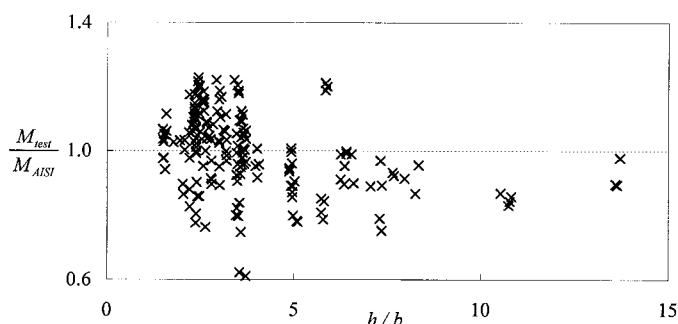


FIG. 12. Performance of AISI Specification versus h/b

(1992) are deemed to have poor applicability. Desmond's and Winter's tests use back-to-back webs, which provide an unrealistic rotational restraint. Ellifritt et al.'s (1992) tests primarily fail in the lateral-torsional mode. Elhouar and Murray's (1985) summary of proprietary tests does not provide enough detailed information on loading and bracing.

The majority of the remaining tests are on face-to-face channels in two-point bending. The channels typically have significant bracing at the load application point as well as a regularly spaced angle or bar attached across the two channels in both the compression flange and the tension flange. The bracing is to insure that lateral-torsional buckling does not occur and to approximate the effect of sheeting. The small spacing of the attached angles or bars (often 300 mm ~12 in. or 150 mm ~6 in.) partially restricts the distortional mode.

If the bracing length (L_b) is less than the predicted L_{cr} from (41), then L_b is used in determining the distortional buckling stress. In many tests $L_b < L_{cr}$. Therefore capacity lower than the experimentally observed strength is possible even for a laterally braced member, because of the fact that the distortional mode is partially restricted.

The flexural capacity of the remaining test data is assessed via the AISI specification (M_{AISI}) and the two proposed methods M_1 and M_2 (Table 5). The statistical results are summarized in Table 6. One striking feature that Table 6 does not bring out is the systematic error that exists in the current AISI specification method for large h/b values (Fig. 12).

From Table 6, the overall performance of the AISI specification method appears adequate. A more detailed analysis reveals several inadequacies. For one, several of the individual tests groups yield consistently unconservative predictions ($n < 1$). Second, the systematic error for large h/b is problematic. Third, the AISI method is not a function of bracing length. Therefore, the same members at longer unbraced lengths (but members still not failing in lateral-torsional buckling) have the same strength prediction via the AISI specification. This is inadequate—until L_b exceeds L_{cr} , the distortional buckling stress and the strength will decrease.

An integrated design method that employs local and distortional buckling calculations is possible and reliable. The systematic error for large h/b values observed in the AISI specification is alleviated in either of the proposed methods (M_1 or M_2). The test to predicted ratio is slightly on the conservative side (>1) for the overall results of the proposed models. The standard deviation and number of unconservative predictions are both lower than the AISI specification for the overall results.

Often, including the local buckling interaction (M_2) actually yields a more conservative prediction than that determined by ignoring it and using an element approach (M_1). However, individual cases are observed where including the local buckling interaction yields markedly better results. Local buckling initiated by long edge stiffeners and local buckling with highly slender webs and compact flanges are examples where including the interaction is observed to improve the strength prediction markedly.

CONCLUSIONS

Laterally braced cold-formed steel flexural members with edge stiffened flanges have two important buckling phenomena: local and distortional. Current AISI specification methods do not explicitly treat the distortional mode. Distortional buckling deserves special attention because it has the ability to control the final failure mechanism in many cases and is observed to have a lower postbuckling capacity than local buckling. New hand methods are developed to predict the critical buckling stress in both the local and the distortional mode. A design method for strength prediction, based on the unified effective width approach, is developed. The design method uses the new expressions for prediction of the local and distortional buckling stress and also introduces a new approach for determining the effective width of the web. The resulting design method is compared with a large body of experimental results and is shown to provide more consistent and conservative prediction than the existing AISI specification. Proper incorporation of the distortional buckling phenomena is imperative for accurate strength prediction of cold-formed steel members.

ACKNOWLEDGMENTS

The sponsorship of the AISI in conducting this research is gratefully acknowledged.

APPENDIX I. REFERENCES

- American Iron and Steel Institute (AISI). (1996). *AISI specification for the design of cold-formed steel structural members*. American Iron and Steel Institute, Washington, D.C.
- Canadian Standards Association. (1994). *S136-M94 cold-formed steel structural members*, Rexdale (Toronto), ON, Canada.
- Cheung, Y. K. (1976). *Finite strip method in structural analysis*. Pergamon, Pergamon, New York.
- Cohen, J. M. (1987). "Local buckling behavior of plate elements." *Dept. of Struct. Engrg. Rep.*, Cornell University, Ithaca, N.Y.
- Davies, J. M., and Jiang, C. (1996). "Design of thin-walled beams for distortional buckling." *Proc., 13th Int. Spec. Conf. on Cold-Formed Steel Struct.*, W. W. Yu and R. A. Laboube eds., University of Missouri, Rolla, Mo., 141–154.
- Desmond, T. P., Peköz, T., and Winter, G. (1981). "Edge stiffeners for thin-walled members." *J. Struct. Div.*, ASCE, 107, 329–353.
- Elhouar, S., and Murray, T. M. (1985). "Adequacy of proposed AISI effective width specification provisions for Z- and C-purlin design." *Rep. No. FSEL/MBMA 85-04*, Fears Structural Engineering Laboratory, University of Oklahoma, Norman, Okla.
- Ellifritt, D., Glover, G., and Hren, J. (1997). "Distortional buckling of channels and zees not attached to sheathing." *Rep. No. 4504530-12*, American Iron and Steel Institute, Washington, D.C.
- Ellifritt, D., Sputo, T., and Haynes, J. (1992). "Flexural capacity of discretely braced C's and Z's." *Proc., 11th Int. Spec. Conf. on Cold-Formed Steel Struct.*, W. W. Yu and R. A. Laboube eds., University of Missouri, Rolla, Mo., 109–129.
- Hancock, G. J. (1995). "Design for distortional buckling of flexural members." *Proc., 3rd Int. Conf. on Steel and Aluminum Struct.*, G. A. Aşkar, ed., Boğaziçi University, Istanbul, Turkey, 275–284.
- Hancock, G. J. (1997). "Design for distortional buckling of flexural members." *Thin-Walled Struct.*, 27(1), 3–12.
- Hancock, G. J., Kwon, Y. B., and Bernard, E. S. (1994). "Strength design curves for thin-walled sections undergoing distortional buckling." *J. Constr. Steel Res.*, 31(2-3), 169–186.
- Hancock, G. J., Rogers, C. A., and Schuster, R. M. (1996). "Comparison of the distortional buckling method for flexural members with tests." *Proc., 13th Int. Spec. Conf. on Cold-Formed Steel Struct.*, W. W. Yu and R. A. Laboube eds., University of Missouri, Rolla, Mo., 125–140.
- Hibbitt, Karlsson & Sorensen, Inc. (HKS). (1995). *ABAQUS version 5.5*. Hibbitt, Karlsson & Sorensen, Pawtucket, R.I.
- LaBoube, R. A., and Yu, W. (1978). "Structural behavior of beam webs subjected to bending stress." *Civil engineering study structural series, Rep. 78-1*, Department of Civil Engineering, University of Missouri-Rolla, Rolla, Mo.
- Lau, S. C. W. (1988). "Distortional buckling of thin-walled columns." PhD thesis, University of Sydney, Sydney, Australia.
- Lau, S. C. W., and Hancock, G. J. (1987). "Distortional buckling formulas for channel columns." *J. Struct. Engrg.*, ASCE, 113(5), 1063–1078.

- Moreyra, M. E. (1993). "The behavior of cold-formed lipped channels under bending," MS thesis, Cornell University, Ithaca, N.Y.
- Peköz, T. (1987). "Development of a unified approach to the design of cold-formed steel members." *AISI Res. Rep. No. CF 87-1*, American Iron and Steel Institute, Washington, D.C.
- Rogers, C. A., and Schuster, R. M. (1995). "Interaction buckling of flange, edge stiffener and web of C-sections in bending." *Res. Into Cold Formed Steel, Final Rep. of CSSBI/IRAP Proj.*, Department of Civil Engineering, University of Waterloo, Waterloo, Canada.
- Schafer, B. W., and Peköz, T. P. (1998). "Computational modeling of cold-formed steel: Characterizing geometric imperfections and residual stresses." *J. Const. Steel Res.*, 47(3), 193–210.
- Schardt, R., and Schrade, W. (1982). *Kaltprofil-Pfetten*. Institut Für Statik, Technische Hochschule Darmstadt, Bericht Nr. 1, Darmstadt, Germany (in German).
- Schuster, R. M. (1992). "Testing of perforated C-stud sections in bending." *Report for the Canadian Sheet Steel Building Institute*, University of Waterloo, Waterloo, ON, Canada.
- Seah, L. K., and Rhodes, J. (1993). "Simplified buckling analysis of plate with compound edge stiffeners." *J. Engrg. Mech.*, ASCE, 119(1), 19–38.
- Shan, M., LaBoube, R. A., and Yu, W. (1994). "Behavior of web elements with openings subjected to bending, shear and the combination of bending and shear." *Civil Engineering Study Structural Series, Rep. 94-2*, Department of Civil Engineering, University of Missouri-Rolla, Rolla, Mo.
- Sharp, M. L. (1966). "Longitudinal stiffeners for compression members." *J. Struct. Div.*, ASCE, 102, 187–211.
- von Kármán, T., Sechler, E. E., and Donnell, L. H. (1932). "The strength of thin plates in compression." *Trans. ASME*, 54, 53–57.
- Willis, C. T., and Wallace, B. (1990). "Behavior of cold-formed steel purlins under gravity loading." *J. Struct. Engrg.*, ASCE, 116(8), 2061–2069.
- Winter, G. (1947). "Strength of thin steel compression flanges." *Trans. ASCE, Paper No. 2305*, 112, 1–50.

APPENDIX II. NOTATION

The following symbols are used in this paper:

- b = flange width;
 b_e = effective flange width;

- D = plate rigidity;
 f = stress;
 f_1 = edge stress on an element;
 f_2 = edge stress on an element;
 f_{cr} = minimum buckling stress;
 f_u = ultimate failure stress for a member;
 f_y = material yield stress;
 h = web height;
 h_t = portion of web in tension;
 h_1 = portion of effective width of a web;
 h_2 = portion of effective width of a web;
 k = plate buckling coefficient;
 k_ϕ = rotational stiffness at web flange juncture;
 $k_{\phi fe}$ = elastic rotational stiffness of flange;
 $k_{\phi fg}$ = geometric rotational stiffness of flange;
 $k_{\phi we}$ = elastic rotational stiffness of web;
 $k_{\phi wg}$ = geometric rotational stiffness of web;
 k_{xf} = flange model spring stiffness in x -direction;
 k_{yf} = flange model spring stiffness in y -direction;
 $k_{\phi g} = k_{\phi g}/f$;
 L = length;
 L_b = unbraced length;
 L_{cr} = length at which f is a minimum;
 M = moment;
 \underline{M} = consistent nodal moment;
 M_1 = moment capacity by proposed method 1;
 M_2 = moment capacity by proposed method 2;
 M_{AISI} = moment capacity by AISI specification;
 R_d = reduction factor for distortional buckling stress;
 t = thickness;
 u = flange model displacement in x ;
 v = flange model displacement in y ;
 θ = orientation angle of the edge stiffener (lip);
 λ = slenderness;
 ξ = stress gradient;
 ρ = postbuckling reduction factor; and
 ϕ = flange model twist.